INTERNATIONAL JOURNAL OF CLIMATOLOGY, VOL. 12, 481–497 (1992) 551.551.8:551.510.42:551.584.5(711)

THE SUBURBAN ENERGY BALANCE: METHODOLOGICAL CONSIDERATIONS AND RESULTS FOR A MID-LATITUDE WEST COAST CITY UNDER WINTER AND SPRING CONDITIONS

C. S. B. GRIMMOND

Climate and Meteorology Program, Department of Geography, Indiana University, Bloomington, Indiana 47405, USA

Received 17 May 1991
Accepted 3 March 1992

ABSTRACT

Previous measurements of the urban energy balance primarily have been conducted in summertime. This paper reports the first extended set of winter–spring-time energy balance measurements for a city. The study was conducted in a suburb of Vancouver, British Columbia, from January to June 1987. It included hourly measurements of net all-wave radiation, sensible heat flux and the Bowen ratio. The anthropogenic and storage heat fluxes were modelled. A dynamic source area model was employed to ensure the modelled parameters were consistent spatially with the measured turbulent fluxes. The winter–spring urban energy balances observed in this study are different to those reported for summertime conditions at the same site. The fluxes for the entire period are not symmetrical about solar noon. Hence earlier interpretations possibly should be modified. Apart from this feature the spring season balances are similar to those reported for the summertime in terms of relative importance of individual fluxes. The wintertime energy balance appears to be different to that of spring and summer. The most noticeable feature is the increased importance of the latent heat flux, which on average is the largest output flux in the balance. A secondary, more expected feature, is the increased importance of anthropogenic heat flux as an input in winter.

KEY WORDS Energy balance Urban Anthropogenic heat flux Latent heat flux Sensible heat flux Storage heat flux

INTRODUCTION

Knowledge of the surface energy balance is considered fundamental to an understanding of the boundary layer meteorology and climatology of any site. The surface energy balance of an extensive urbanized surface is defined for a volume that contains the elements of the surface 'canopy', the air between the canopy elements, and the soil down to a depth sufficient to ensure that vertical heat exchange is negligible over the period of interest. Fluxes are determined per unit area of the top of the volume. A fuller explanation of this concept is given by Oke (1988). The surface energy balance may be written:

$$Q^* + Q_F = Q_H + Q_E + \Delta Q_S + \Delta Q_A \quad (\mathrm{W\ m^{-2}}) \tag{1}$$

where all terms are flux densities; Q^* is the net all-wave radiation; Q_F the anthropogenic heat; Q_H the sensible heat; Q_E the latent heat; ΔQ_S the net heat storage; and ΔQ_A the net heat advection. Positive values on the left side of equation (1) are inputs to the system, positive values on the right side are outputs.

Construction of valid energy balances for spatially non-uniform surfaces, such as cities, requires that all component fluxes represent identical source areas. This is particularly important when measured and modelled fluxes are to be combined within an energy balance. If each term in equation (1) is obtained separately, the balance can close only if each term refers to the same system. The surface area influencing the measurement of one term must be the same as that influencing any other term, whether it is measured or modelled, otherwise the energy balance equation is internally inconsistent. The surface area contributing to a flux measurement is termed the 'source area' by Schmid and Oke (1990). The shape and size of the source area

0899–8418/92/050481–17$13.50

is dependent firstly on the process involved, secondly on the instrument used for the measurement, and thirdly on the conditions under which the measurement is performed. The equivalent of the source area in the case of a modelled flux is the model domain, i.e. the surface portion that contains all the characteristics considered in the model. It follows that the source areas of each measured term and the domains of each modelled term must be equivalent for a spatially consistent surface-energy balance.

The objective of this paper is to utilize the source area concept in combining measurement and modelling to investigate urban energy balance fluxes under winter and spring conditions. The scale of the flux determinations relate to an area of suburban land use; i.e. at the local scale (Oke, 1984), rather than from individual surfaces, such as lawn or road. The state of urban energy balance research has been reviewed by Oke (1988). Except for Kerschgens and Drauschke's (1986) two-day winter field study in Bonn, Germany, most urban energy balance measurements have been conducted in summer. This study probably is the first to report measured fluxes for an extended period of winter and spring conditions.

DETERMINATION OF HOURLY ENERGY BALANCES

In this study hourly energy balance fluxes are determined for a site (called Sunset) in a suburban area of Vancouver, British Columbia, using measurements of Q^*, Q_H and Q_E, and modelled values of Q_F and ΔQ_S, ΔQ_A is omitted on the basis of Steyn's (1985) analysis of data from the same tower. He showed energy residuals from overdetermined balances are zero in the mean, and are unrelated to wind speed or direction. This strongly suggests that the Sunset site is not characterized by systematic local-scale advection. This conclusion is further supported by the small spatial variability found by Schmid *et al.* (1991) when comparing observations on the fixed tower at Sunset with those from a mobile tower operated at several sites within a 2-km radius.

Physical setting and climatology of Vancouver during the study period

Observations were conducted in the Sunset suburb, Vancouver (49°15′N, 123°18′W; Figure 1). Vancouver is located on the west coast of North America, but is climatically isolated from the continental interior by a series of mountain chains paralleling the coastline. It is sheltered from the Pacific Ocean by Vancouver Island. The city is situated at the west end of the Lower Fraser Valley and has low to moderate relief. The Sunset neighbourhood is predominantly composed of one- and two-storey single family dwellings. The area has a slight south-westerly slope towards the Fraser River.

The general climatology of Vancouver is described in Hay and Oke (1976), the following is a brief description. The large-scale upper level flow generally is from the westerly quarter, off the Pacific. Embedded in this flow are disturbances (cyclones), which are best developed and most frequent in winter. High-pressure (anticyclonic) regimes have a relatively low frequency in the winter months, because normally they are unable to withstand the invasion of vigorous cyclonic disturbances. Summer brings an extension of the Pacific anticyclone regime into the mid-latitudes, resulting in the predominance of generally cloudless, warm weather with light flow.

Several physical features of the landscape combine to produce local climate variations. Chief among these are the influences of topography, proximity to the ocean, and urbanization. The setting of Vancouver leads to the occurrence of land–sea and mountain–valley circulations. The land/sea breeze causes predominantly westerly winds during daytime and weaker easterly flow during the night. It has a higher frequency during the summertime (Steyn and Faulkner, 1986). Owing to the sea breeze and the associated advection of marine air, the height of the daytime planetary boundary layer typically is reduced to only 500 m or less (Steyn and Oke, 1982; Steyn and McKendry, 1988; Cleugh, 1990).

Measurements were conducted from Year Day (Y/D) 87/21 (21 January) to 87/179 (28 June 1987). The monthly average climate statistics collected by the Canadian Atmospheric Environment Service at the Vancouver International Airport Climate Station (Fig. 1) indicate that, in general, the measurement period was warmer than normal, had a greater number of sunshine hours, but had almost normal precipitation (more as rain and less as snow than normal).

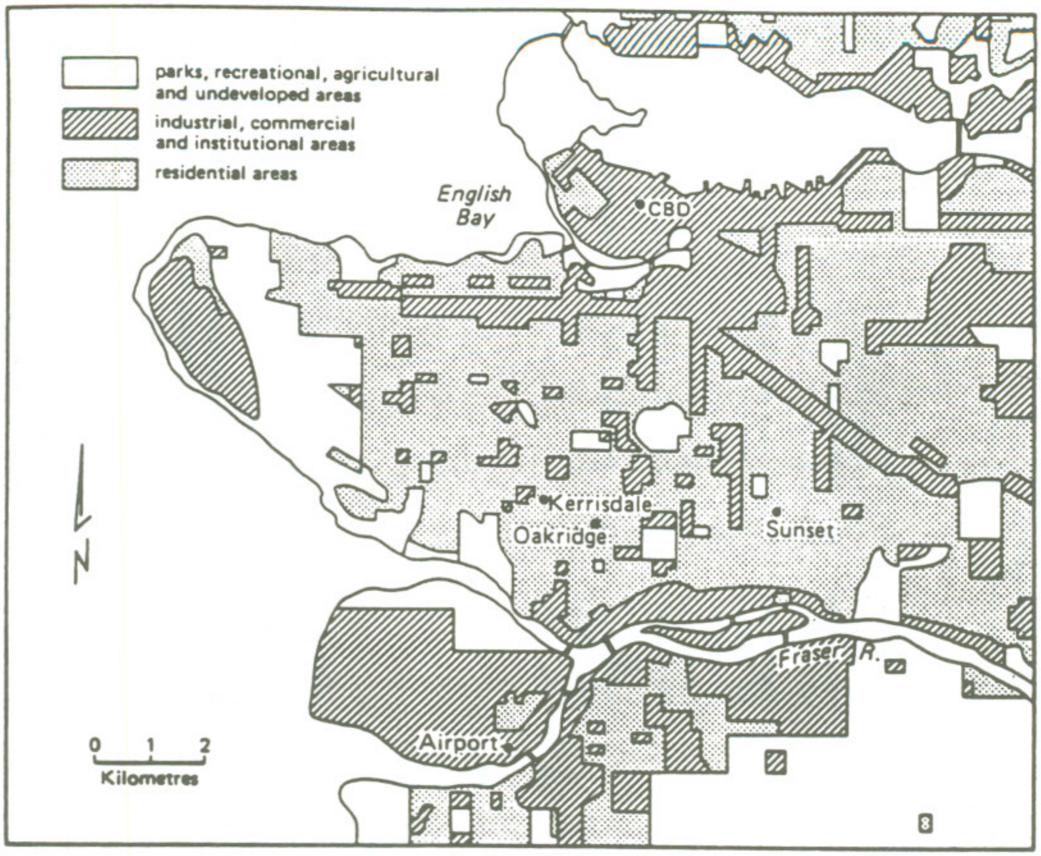

Figure 1. The location of the Sunset site in Vancouver and the surrounding land use

Measured fluxes

To obtain fluxes representative of the local scale, measurements must be made well above the height of the roughness elements to ensure that observations are conducted in the surface layer, so that they represent the integrated effects of the surface types that characterize the land use (Oke *et al.*, 1989).

Roth *et al.* (1989) report a study of the turbulence spectra of temperature, the vertical and longitudinal wind components as well as the cospectra of the fluxes of sensible heat and momentum at the Sunset site, including an assessment of whether the measurement height used is above the roughness sublayer. In accord with their findings a sensor height of >20 m above zero plane displacement, and an averaging time of 60 minutes were selected for the present study. The zero plane displacement and roughness lengths of the Sunset site were determined by Steyn (1980) to be 3·5 m and 0·52 m, respectively.

The variables measured, details of the instrumentation used and their positions on the tower are presented in Table I. The signals were logged on Campbell Scientific Inc CR21X data loggers. All times referred to are local apparent time (LAT).

From the data collected from the RTDMS (see Table I) β was calculated:

$$\beta = [\gamma(\Delta T_d + \Gamma \Delta z)]/[(s+\gamma)\Delta T_W - \gamma \Delta T_d] \quad (2)$$

where ΔT_d is the dry-bulb temperature difference (°C); ΔT_W the wet-bulb temperature difference (°C); Γ the dry adiabatic lapse rate (°C m^{-1}); s the slope of the saturation vapour pressure curve at T_W (Pa °C^{-1}), calculated using Lowe (1977); γ the psychrometric constant (Pa °C^{-1}), calculated using Fritschen and Gay (1979) with

Table I. Instrumentation specifications for the measurements

Flux	Instrument manufacturer, model	Height[a] (m)	Comments
Net all-wave radiation Q^*	Net pyrradiometer Swissteco S1	20·5	Polythene domes: inflated and kept free of internal condensation by air pumped through granulated silica desiccant Instantaneous error: 3–4% (Latimer, 1972) Hourly error: 5% (Cleugh and Oke, 1986)
Sensible heat flux Q_H	Sonic anemometer and fine wire thermocouple system (SAT) Campbell Scientific CA27	20·5	Vertical wind velocity: phase shift in the sound wave Air temperature: fine-wire thermocouple (diameter 12·7 μm) Sample rate: 10 Hz Covariances: 15-minute periods Hourly flux: mean of four 15-minute values Measurement errors: Tanner (CSI, pers. comm., 1987): measurement error $<10\%$; Roth *et al.* (1989): system measures $w'T'$ adequately; Schmid *et al.* (1991): intercomparison of two instruments for hourly flux RMSE $= 12\ \mathrm{W\,m^{-2}}$
Wind speed u	Cup anemometer Met-One 012A	19	
Wind direction φ	Wind vane Met-One 024A	19	
Relative humidity Temperature rh and T	Relative humidity probe Rotronics Instrument Corp. MP-100	19	
Dry bulb and wet bulb temperature T_d and T_W	Reversing temperature difference measurement system (RTDMS) Similar to McCaughey *et al.* (1987)	17·2 10·1	Used to determine Bowen ratio ($\beta = Q_H/Q_E$) Temperature: 10 junction copper/constantan thermopiles, mounted within aspirated shields on two carts that move up and down on a trackway Cart separation: 7·1 m Reversal: twice per hour—ten minutes to travel (<4 minutes) and equilibrate at the new level. 20 minutes at each level-providing two 10-minute means
Precipitation P	Rain gauge Meteorolog. Res. Inc 382B		

[a] Effective height of instruments. The instruments were mounted on a 29-m triangular-section steel lattice, free-standing tower. The base of the tower is 5 m below the level of a surrounding embankment. Therefore the maximum effective height of the tower is 20·5 m (height of instruments minus zero plane displacement and embankment).

latent heat of vaporization calculated using Henderson-Sellers (1984); and Δz the sensor separation (m). Using this system Q_H can be determined from β using the energy balance:

$$Q_{H\beta}=[\beta(Q^*+Q_F-\Delta Q_S)]/(1+\beta) \tag{3}$$

and similarly the latent heat flux (Q_E) can be determined:

$$Q_{E\beta}=(Q^*+Q_F-\Delta Q_S)/(1+\beta) \tag{4}$$

Alternatively, Q_E can be calculated using β and Q_H measured with the SAT (see Table I): $Q_E=Q_H/\beta$.

The error analysis used to determine the precision of the RTDMS follows the procedure of Kalanda (1979). Using this method maximum errors were determined for the temperature differences, absolute temperatures, β, $Q_{H\beta}$ and $Q_{E\beta}$. The errors calculated for each hour were used to stratify the data to decide whether the Bowen-ratio–energy-balance or the SAT–energy-balance method should be used to determine the 'measured' Q_E.

For some hours there is more than one method of obtaining the Q_H and Q_E fluxes. In the case of Q_H, eddy correlation measurements were used preferentially (Q_H); otherwise, it was obtained using equation (3) ($Q_{H\beta}$). If the resulting $Q_{H\beta}$ and latent heat fluxes ($Q_{E\beta}$) were realistic and the error in $Q_{H\beta}$ and $Q_{E\beta}$ were less than 30 per cent, or if the absolute size of both fluxes was less than 20 W m^{-2}, then the calculated fluxes were accepted.

The method used for Q_E is dependent on that used for Q_H. If Q_H from the SAT was available then it was determined as a residual (Q_{ER}) from equation (1). Otherwise it was calculated from equation (4) ($Q_{E\beta}$). The hours when this was used are the same as those for $Q_{H\beta}$. The reason for choosing to accept Q_H and Q_{ER} first rather than following a procedure of determining an optimum energy balance, such as that suggested by Steyn (1985), is based on the expectation that this procedure will produce the smallest error in the turbulent fluxes.

Results of a statistical and graphical comparison of the turbulent sensible heat flux densities determined by eddy correlation (Q_H) and Bowen-ratio–energy-balance ($Q_{H\beta}$) are similar to those reported by Cleugh and Oke (1986) for a rural site. Here the comparison is broken down by error in β (Table II). Only 8 h of the simultaneous measurements had a maximum error of less than 10 per cent. These values, except for one point, are virtually identical. As the error increases (beyond 20 per cent) the number of extreme outliers does not increase. At $\leqslant 100$ per cent error there is a noticeable increase in values close to zero; in particular, values of $Q_{H\beta}$ are calculated as almost equal to zero, whereas for the same hours Q_H have a greater range.

Modelled fluxes

Given that the radiative field is relatively uniform in space (Schmid *et al.*, 1991) it is appropriate to match all modelled fluxes (in this study Q_F and ΔQ_S) to the source areas for the turbulent fluxes since these are variable. To ensure that the energy balance is consistent for an hour when fluxes are both modelled and measured the turbulent source areas are imposed on a geographic information system containing the surface characteristics necessary to calculate the spatially corresponding anthropogenic and storage fluxes. This allows the surface description for modelling purposes to vary dynamically with meteorological conditions (wind directions, stability, etc.), hence with the measurements.

The dimensions of the elliptically shaped source area are determined using the Schmid and Oke (1990) Source Area Model (SAM). The SAM output consists of weighted elliptically shaped source areas for each hour with dimensions that are a fairly sensitive function of sensor height, and are further affected by stability and roughness, in that order of importance. All source area dimensions increase as the stability changes from unstable to neutral to stable conditions (Pasquill, 1972). The area between each ellipse has equal weight (see Grimmond and Oke 1991, figure 2). Utilizing the meteorologically controlled SAM ellipses with a data base (Appendix I) it is possible to assign objectively the values to parameters necessary for consistent flux calculations. The relation between the components are:

Meteorological conditions	→	Source Area Model (SAM)	→	Database accessing system	→	Surface Database	→	Model parameters	→	Flux Model

Table II. Comparison of Q_H and $Q_{H\beta}$ (W m^{-2}) with varying errors in β[a]

Per centage error in β	n	$Q_{H\beta}$ Mean	$Q_{H\beta}$ SD	Q_H Mean	Q_H SD	RMSE (W m^{-2})	MAE (W m^{-2})	m_f	r^2
<10	8	32·2	35·9	35·4	52·6	23·4	13·7		
<20	499	170·2	93·7	139·9	88·9	68·1	52·0	1·34	0·58
<30	683	149·3	94·8	122·9	72·1	67·0	72·1	1·31	0·58
<40	777	136·8	96·5	114·2	74·0	64·9	47·5	1·30	0·60
<50	846	128·8	97·4	107·6	75·2	63·1	45·7	1·30	0·63
<60	890	123·5	98·2	103·7	76·0	62·2	44·6	1·29	0·64
<70	948	117·2	99·3	98·5	76·8	61·0	43·2	1·29	0·66
<80	991	112·8	99·5	95·2	77·1	60·0	42·2	1·28	0·67
<90	1033	108·6	99·7	92·3	77·5	59·6	41·7	1·28	0·67
<100	1079	104·1	99·9	88·9	77·9	59·0	40·9	1·27	0·68

[a] n = number of hours; SD = standard deviation; RMSE = root-mean-square error; MAE = mean absolute error; r^2 = coefficient of determination; m_f = slope of linear functional relationship (Mark and Church, 1977).

Storage heat flux. ΔQ_S, the net uptake or release of energy from the urban system, cannot be measured directly. An objective hysteresis model that has been tested over a range of meteorological conditions is used to calculate ΔQ_S (Grimmond *et al.*, 1991). The general form of the equation is:

$$\Delta Q_S = \sum_{i=1}^{n} \left[a_{1i}(Q^* + Q_F) + a_{2i}\frac{\partial(Q^* + Q_F)}{\partial t} + a_{3i} \right] \tag{5}$$

where, when $\Delta t = 1$, $\partial(Q^* + Q_F)/\partial t = 0{\cdot}5[(Q^* + Q_F)_{t+1} - (Q^* + Q_F)_{t-1}] \cdot \partial(Q^* + Q_F)/\partial t$ has units of W m^{-2} h^{-1}; and the coefficients a_1, a_2, and a_3 are dimensionless, h, and W m^{-2} respectively. The model parameters (a_1, a_2, a_3) relate to the surface characteristics, which are weighted by their proportional presence (i). These are calculated using the SAM weighted ellipses and the geographic data base (Appendix I).

Anthropogenic heat flux. Q_F, the energy released owing to human activities, is often regarded as negligible or is ignored in urban energy balance studies. This is due to two factors, both of which are related to the fact that most previous studies have been conducted under summer conditions. Firstly, in many urban areas in the mid- and high latitudes the absolute size of Q_F is smaller in summer than in winter. Secondly, even if this is not the case in the summertime the magnitude of the other fluxes are larger and therefore the relative importance of Q_F is smaller. Its magnitude may be of the order of the error of measurements only. In this study of the seasonal nature of the energy balance of a temperate city, its magnitude and relative importance in the balance can become important and must be considered.

Q_F may be subdivided into three components (Bach, 1970):

$$Q_F = Q_{FV} + Q_{FH} + Q_{FM} \qquad (\text{W m}^{-2}) \tag{6}$$

where Q_{FV} is the heat produced by combustion of vehicle fuels: Q_{FH} is released from 'stationary sources' (primarily within buildings); and Q_{FM} is the heat released by metabolism (often negligible when compared with the other two components, but incorporated in this study for completeness). Q_F cannot be measured directly. Appendix II outlines the methods used to approximate Q_F on an hourly basis.

Figure 2 shows the daily trend of the three Q_F components and their combined total for YD 87/22 using a 2-km radius circle centred on the Sunset site to determine the required mean surface parameters. The influence of the morning and afternoon rush hours are apparent in the Q_{FV} and Q_F profiles, and the slightly out of phase peaks in Q_{FH}. Q_{FM} is small and shows a step transition between the 'sleep' and 'active' periods of the day. In the summer in Vancouver Q_{FH} is reduced but Q_{FV} remains approximately the same.

Consideration needs to be given to the inclusion of the Q_F term in the energy balance. Some of the measured terms of the energy balance include portions of the anthropogenic heat release so there is some danger of 'double counting'. On the output side of the energy balance, the measured fluxes already will incorporate the effect of Q_F. A portion of Q_F is incorporated in measurements of Q_H (using the SAT) and RTDMS temperatures. Measurements of Q^*, also, partially include Q_F because it affects the longwave exchange portion of Q^* via the surface temperature (T_S):

$$L\uparrow = \varepsilon\sigma T_S^4 \tag{7}$$

$$Q^* = K^* + (L\downarrow - L\uparrow) \qquad (\mathrm{W\,m^{-2}}) \tag{8}$$

where $L\uparrow$ is the longwave radiation emitted from the surface; ε the emissivity of the surface materials; and σ the Stefan-Boltzmann constant ($\mathrm{W\,m^{-2}\,K^{-4}}$); K^* the net shortwave radiation; and $L\downarrow$ the longwave radiation received at the surface ($\mathrm{W\,m^{-2}}$). Q_F causes an increase in T_S which leads to an increase in $L\uparrow$. The increase in T_S, and therefore the effect on Q^*, is a function of the heat capacity of the building fabric, the three-dimensional surface area of the building, and the amount of energy released within the building. The effect on temperature can be calculated approximately through the steps outlined in Appendix II. Such calculations indicate that the increase in T_S, as a consequence of Q_F, will be less than 1°C. Within the range 0–40°C, a 1° rise in T_S results in 5–6 $\mathrm{W\,m^{-2}}$ increase in $L\uparrow$. Therefore the measured Q^* flux includes a reduction due to the Q_F flux. In this study Q_F was added directly to the energy balance. Its significance as an energy input to the system is discussed below.

ENERGY BALANCE RESULTS AND DISCUSSION

Measurements have been conducted at the same site as this study by Oke and McCaughey (1983) and Cleugh and Oke (1986) in the summers of 1980 and 1983, respectively. It should be noted that Oke and McCaughey state that the summer of 1983 was an extreme case with respect to evaporation, so the comparisons should be considered in that context. In both studies Q^* was measured in the same manner as here, but Q_F was not included in the energy balnace. Oke and McCaughey (1983) measured β using a reversing differential psychrometer system different to that used in this study (see Kalanda *et al.* (1980) for full details). Oke and McCaughey used the objective linear storage heat flux parameterization (Oke *et al.*, 1981) to obtain ΔQ_S, together with β to calculate Q_H and Q_E. Cleugh and Oke (1986) also used the objective linear storage scheme, but Q_H was measured using a SAT, leaving Q_E as a residual in the energy balance. The difference in methods, especially considering their dependence on ΔQ_S, suggests that the results of the different studies should be compared with caution. The only fluxes directly comparable with the present results are Q^*, and Q_H for 1983.

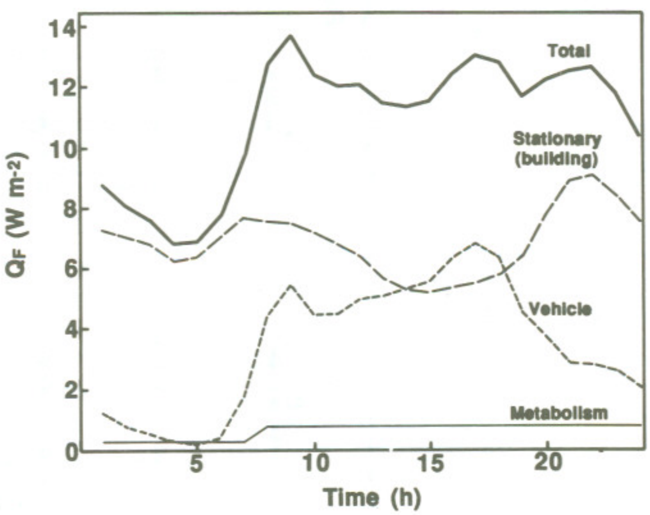

Figure 2. Anthropogenic heat flux for 87/22 with the three components and total hourly flux

It is important to recognize that the instrumentation utilized in this study, in particular the SAT, means that the data is biased to 'non-rain' periods (but does not explicitly exclude periods of rain). The data collected can be stratified by the method used to give six data sets for computations:

M1—complete 24-h days with Q_H via SAT only (56 days);
M2—complete 24-h days with Q_H via SAT and RTDMS (73 days);
M3—complete 24-h days (M2) and days that have 21–23 h for which energy balances can be calculated (99 days);
M4—M3 plus days with 19–20 h of data (109 days);
M5—M4 plus days with <19 h of data (145 days);
M6—all 159 days, however some hours only have Q^* data.

With a transition from method M1 through to M6 the conditions under which the measurements were taken become more diverse and less restricted to 'good' weather, but less complete in terms of full data availability. In order to consider the effect of the measurement method on the individual fluxes the average monthly flux for both daytime ($Q^*>0$) and daily (24 h) data for each method were determined. The values for each flux and method are plotted in Figure 3, with the points representing M4 connected. As would be expected Q^* shows the greatest variability with method as this flux was measured under the widest range of conditions (M6). The daily (24 h) results presented subsequently are calculated using M4. This method represents a trade-off between data quality and completeness, and the greatest range of meteorological conditions. The average energy balance fluxes and ratios of the partitioning of the energy for each month using M4 are presented in Table III.

The diurnal trend of the mean monthly fluxes (using M4) are shown in Figure 4. A time series of the daytime ($Q^*>0$) mean fluxes (in MJ m^{-2} d^{-1}) and the Bowen ratios for the entire period are shown in Figure 5.

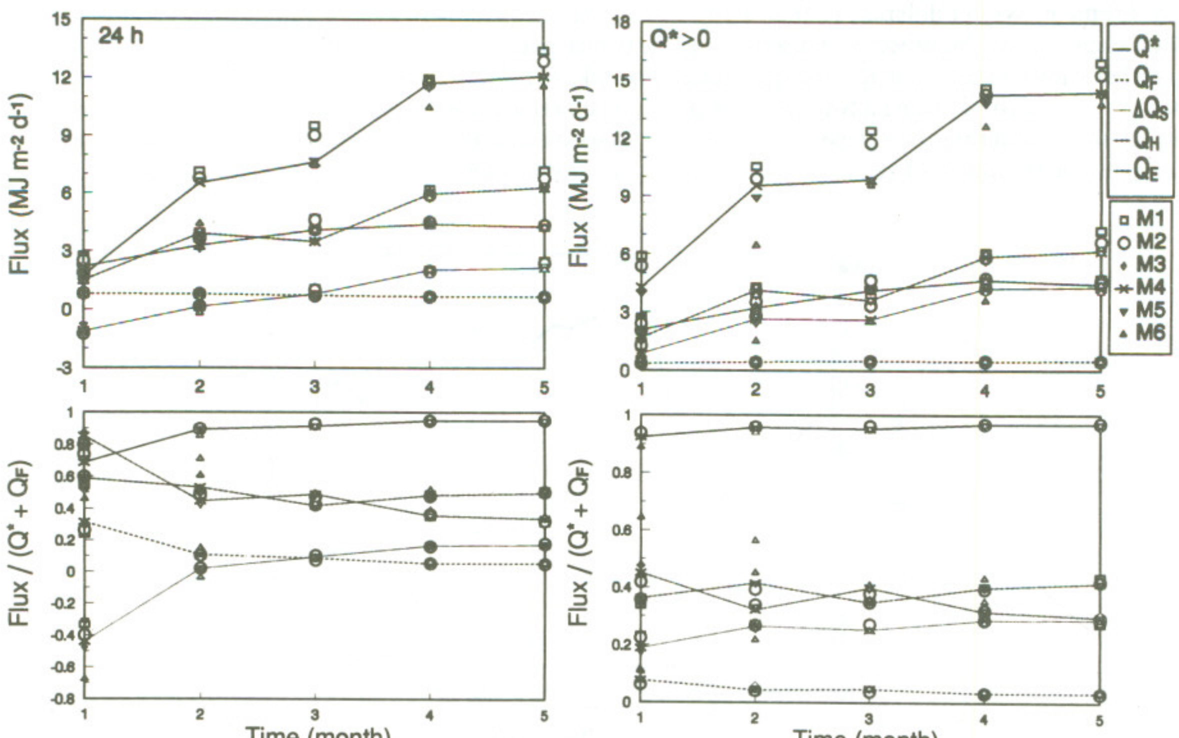

Figure 3. Average monthly energy balance fluxes and their relative proportions for (a) daily (24 h) and (b) daytime ($Q^*>0$)

Table III. Averages of the energy balance fluxes for the measurement period by month

Period	Mean ($MJ\ m^{-2}\ d^{-1}$)											
	Q^*+Q_F	Q^*	Q_F	ΔQ_S	Q_H	Q_E	$\frac{Q^*}{Q^*+Q_F}$	$\frac{Q_F}{Q^*+Q_F}$	$\frac{\Delta Q_S}{Q^*+Q_F}$	$\frac{Q_H}{Q^*+Q_F}$	$\frac{Q_E}{Q^*+Q_F}$	β
(a) Day time: $Q^*>0$												
21–59	4·62	4·27	0·35	0·87	1·67	2·08	0·92	0·07	0·19	0·36	0·45	0·80
60–90	9·95	9·52	0·43	2·63	4·13	3·20	0·96	0·04	0·26	0·42	0·32	1·29
91–120	10·31	9·83	0·48	2·61	3·59	4·11	0·95	0·05	0·25	0·35	0·40	0·87
121–151	14·71	14·24	0·47	4·22	5·85	4·64	0·97	0·03	0·29	0·40	0·33	1·26
152–179	14·84	14·36	0·48	4·28	6·15	4·41	0·97	0·03	0·29	0·42	0·30	1·40
(b) Daytime: $(Q^*+Q_F)>0$												
21–59	4·62	4·22	0·40	0·83	1·66	2·13	0·91	0·09	0·18	0·36	0·46	0·78
60–90	9·95	9·52	0·43	2·63	4·13	3·20	0·96	0·04	0·26	0·42	0·32	1·29
91–120	10·31	9·83	0·48	2·61	3·59	4·11	0·95	0·05	0·25	0·35	0·40	0·87
121–151	14·71	14·24	0·47	4·22	5·85	4·64	0·97	0·03	0·29	0·40	0·32	1·26
152–179	14·86	14·36	0·51	4·15	6·32	4·40	0·97	0·03	0·28	0·43	0·30	1·44
(c) Daily: (24 h)												
21–59	2·56	1·75	0·80	−1·13	1·50	2·18	0·69	0·31	−0·44	0·59	0·85	0·69
60–90	7·31	6·53	0·78	0·14	3·89	3·28	0·89	0·11	0·02	0·53	0·45	1·19
91–120	8·34	7·62	0·72	0·78	3·48	4·08	0·91	0·09	0·09	0·42	0·49	0·85
121–151	12·39	11·73	0·66	2·03	5·97	4·40	0·95	0·05	0·16	0·48	0·36	1·36
152–179	12·74	12·08	0·66	2·16	6·31	4·27	0·95	0·05	0·17	0·50	0·34	1·47

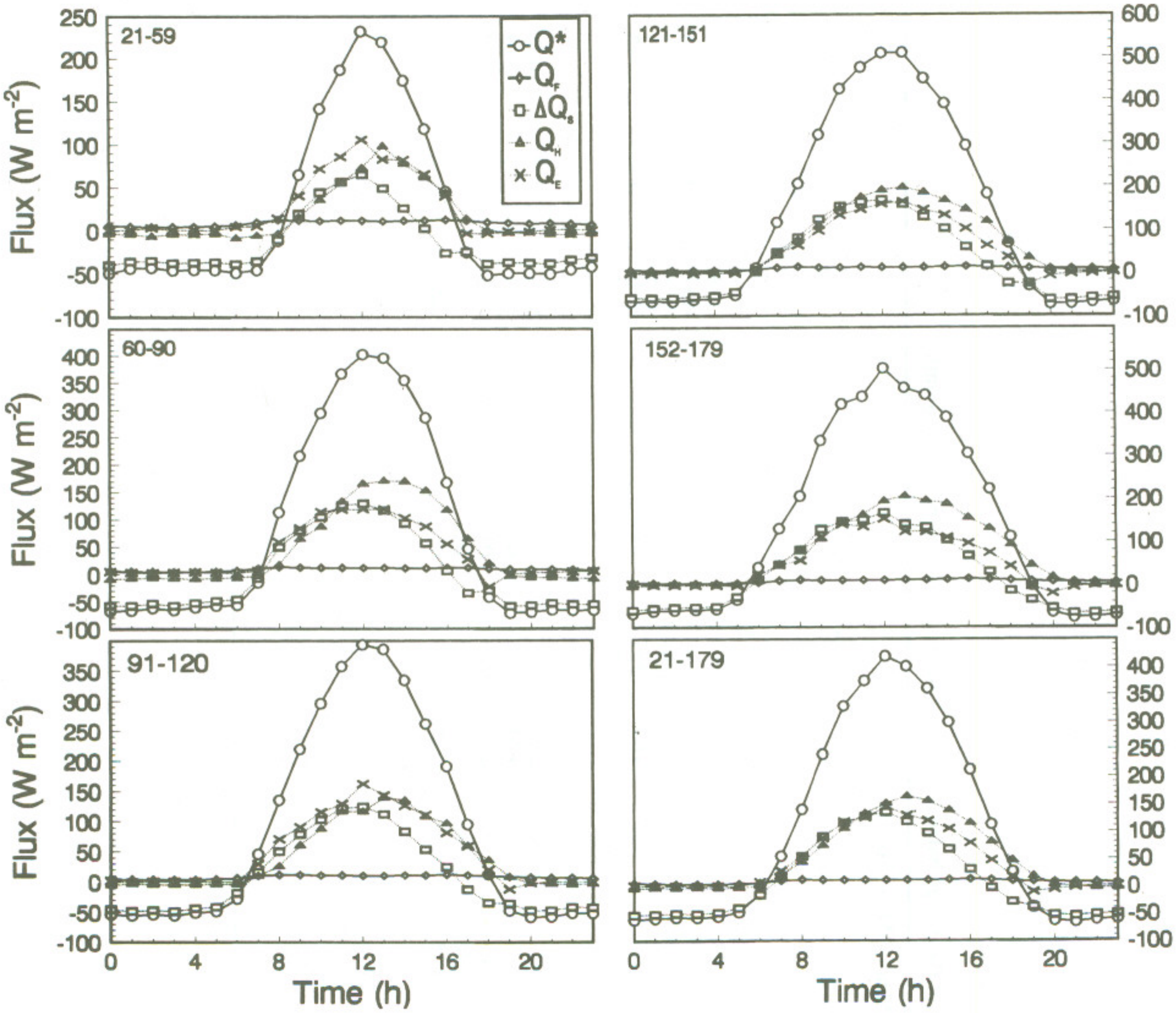

Figure 4. Diurnal trend of monthly hourly average energy balance fluxes for the periods specified in the top left-hand corner of each plot. Note that the vertical scale (flux density with units of W m^{-2}) differs between diagrams

Figures 3–5 and Table III permit a consideration of the relative and absolute trends in each flux and their variability over the extended winter–spring period.

As expected in Vancouver, Q_F decreases in significance and size as Q^* increases from winter to summer. The relative importance is greater for the whole day (24 h) than for the daytime hours [$Q^*>0$ or $(Q^*+Q_F)>0$] (Table III). For the daytime hours it is less than 10 per cent of the energy input (Q^*+Q_F) for all months. When the whole day is considered Q_F contributes more than 10 per cent to the energy balance up until April (Y/D 87/91–120). Therefore it should be considered negligible or can be ignored only if research is being conducted for daytime hours, or if the whole day is under consideration in a non-wintertime study. However, it is probably necessary to pay close attention to the diurnal variability only if a wintertime study is being conducted. Note Vancouver is a city that does not require air conditioning in the summer. Thus the major seasonal change in absolute Q_F is a consequence of reduced heating requirements in the warmer periods. The magnitude and diurnal pattern of the Q_F fluxes are similar to those calculated for other suburban areas (see for

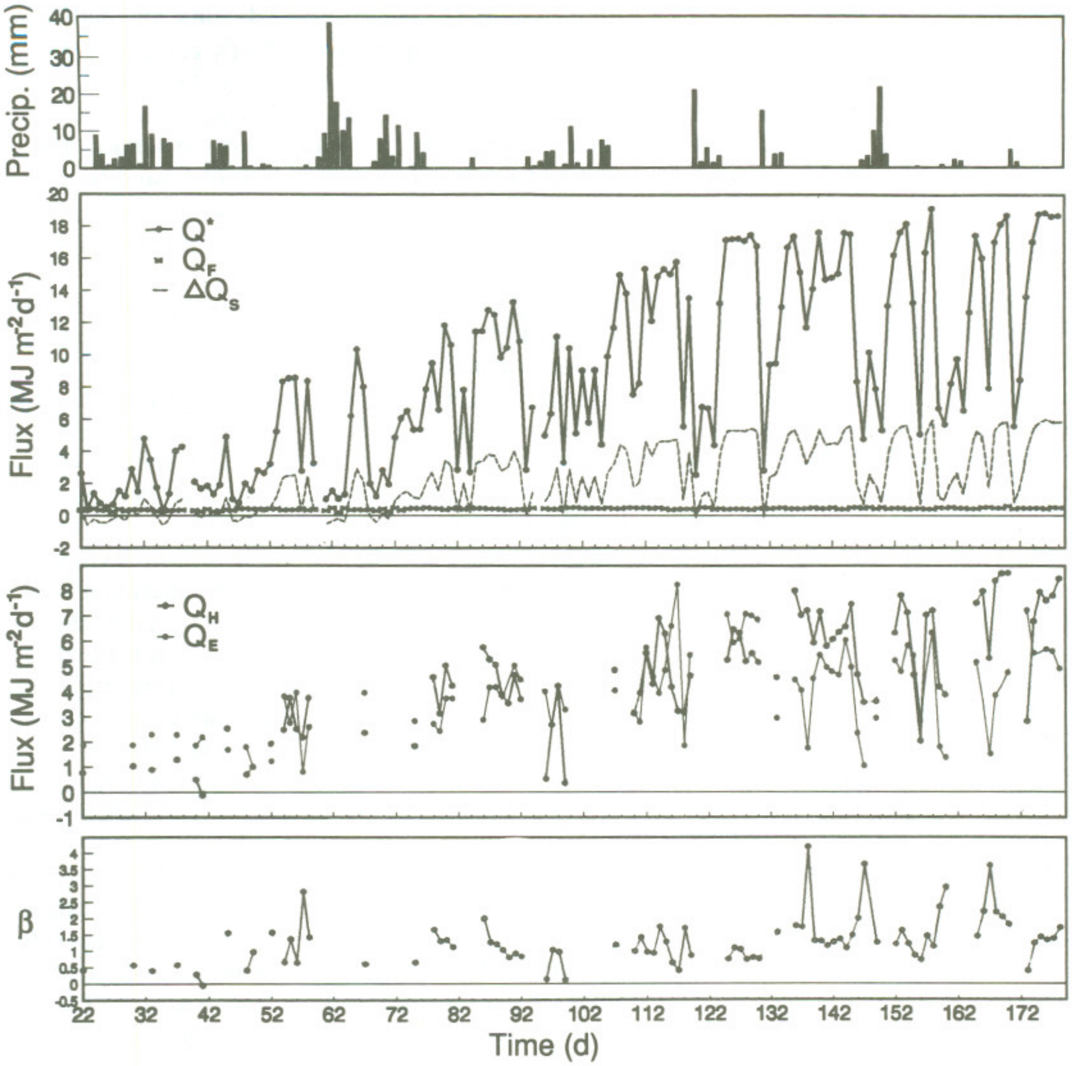

Figure 5. Mean daytime ($Q^*>0$) energy balance fluxes (MJ m^{-2} d^{-1}), Bowen ratio for 87/22-179 and daily precipitation (mm)

example Kalma (1974) or Oke (1988) for a review). The seasonal reduction between winter and summer is similar to other cities that do not have high summertime cooling demands.

The monthly averaged daytime $\Delta Q_S/(Q^*+Q_F)$ ratio increases from 0·18 to 0·28 as Q^* increases. The daytime ratios are higher than those for the previous two summertime studies (Cleugh and Oke = 0·22, Oke and McCaughey = 0·23), except for January–February, but of course different methods were used in 1987. There is a net gain in ΔQ_S for each month except January–February (Figure 3), although there are individual days that do not have a net gain until YD 87/132 (Figure 5). However, the frequency of these days, and the net loss days, drops through time, with none after early March (YD 87/72). The daytime total ΔQ_S mimics the Q^* daytime total pattern (Figure 5) throughout the study period.

The daily and daytime Q_H flux increases with increasing Q^*. The monthly mean daily ratio varies between 0·42 and 0·59 but does not show a distinct seasonal trend (Table III(c)). The daytime ratios vary between 0·36 and 0·43 (Table III(b)). The June value of 0·43 is very similar to the 1983 summertime ratio of 0·44. The 1987 data seem to be more like the 1983 data set than that for 1980.

Q_E in absolute terms, generally, increases with increasing Q^*. However, the daytime and daily Q_E in June 1987 was less than for May, which resulted in a slightly lower proportion of $Q^* + Q_F$ going into Q_E. The trend of the mean monthly daily $Q_E/(Q^* + Q_F)$ ratio shows a decrease from 0·85 in January–February to 0·34 in June (Figure 3). The high ratios in the wintertime are the result of the combination of frequent rain events and small radiation input. Under such conditions the available energy goes first into drying the surface. The daytime $Q_E/(Q^* + Q_F)$ ratios do not show as pronounced a trend as the daily data. The May (0·32) and June (0·30) ratio for 1987 are similar to that for the 1983 data. From Figures 3 and 4 it can be seen that Q_E is an important term in the energy balance in all months. In particular, it is the dominant output flux in the January–February period.

The mean monthly 24-h β (calculated from average Q_H and Q_E fluxes) varies between 0·69 and 1·48 with a mean for the measurement period of 1·17. The daytime ($Q^* > 0$) mean for the measurement period is 1·16 with a range of 0·80–1·40. There is a fairly systematic increase in β with time (Table III, Figure 5) with the exception of the early part of April, reflecting a period of rain. In the early part of the year there are more days when β is < 1 and very few days when it is > 2. By May and June the frequency of days with $\beta < 1$ is very small and there are now blocks of days when it is > 2. On a monthly basis the January–February and April β values are < 1, the remaining months are > 1. The 1983 summertime β lies between the May and June 1987 data. The 1987 mean is close to the typical value of 1 given by Oke (1982) for suburban areas.

The diurnal trend of hourly average fluxes of Q_H, Q_E, and ΔQ_S for the whole measurement period (YD 87/21–179) follow a very similar path until about 1200 LAT (Figure 4: 21–179). In the afternoon Q_H is greater than Q_E which in turn is greater than ΔQ_S. Q_H goes through zero after Q^*, Q_E at approximately the same time as Q^*, and ΔQ_S about 1 h earlier (Figure 4: 21–179). When considered month by month the data for the January–February period (Figure 4: 21–59) stand out as distinct. For this wintertime period Q_E is the most significant output flux in the morning and is the same size as the sensible heat flux in the afternoon. The diurnal trend of the average energy balances for March–June (Figure 4: 60–90, 91–120, 121–151, 152–179) are remarkably similar in form although the size of the fluxes increase. After noon Q_H is the most important output flux. The second most important output flux is consistently Q_E, except for April when it equals Q_H (Figure 4: 91–120).

The fact that the three output fluxes are very similar before solar noon (1200 LAT) (Figure 4) is different from the summertime energy balances reported by Cleugh and Oke (1986), and is due to their calculation of ΔQ_S with a linear function (see above) so that Q_E could be determined as a residual. Measurements from this study, however, indicate that there is an asymmetrical hysteresis relation between 'measured' ΔQ_S (i.e. determined as a residual from measured fluxes) and Q^* (see Grimmond *et al.*, 1991, Figure 8). The difference between these studies, in terms of their diurnal pattern, demonstrates the importance of the storage parameterization, not only in the context of the storage heat flux *per se*, but also because it influences the apparent size of Q_H and Q_E, unless they are determined independently. Except for January–February, the afternoon fluxes generally are similar to those of the Cleugh and Oke study, with Q_H the largest flux, then Q_E, and then ΔQ_S. This suggests that the relative importance of the fluxes remains similar through the spring and summer. However, winter appears to show the greatest difference as noted above. Further winter measurements are needed to document this.

CONCLUSIONS

The results reported here are for a suburban area of a mid-latitude west coast city. The data used to determine the energy balances consist of measured (Q^*, Q_H, Q_E) and modelled (ΔQ_S, Q_F) fluxes. With the available data sources there has been an attempt to maintain consistency between the measurement source area and model domain by use of Source Area Model. It should be noted that the data reported here are amongst the first winter and spring-time measurements.

The winter–spring urban energy balances observed in this study are different from those reported for summertime conditions at the same site. The fluxes for the entire period are not symmetrical about solar noon. Hence earlier interpretations possibly should be modified. Apart from this feature the spring season balances are similar to those reported for the summertime in terms of relative importance of individual fluxes.

The wintertime energy balance appears to be different to that of spring and summer. The most noticeable feature is the increased importance of the latent heat flux, which is in large part due to the temperate maritime climate of Vancouver. On average it is the largest output flux in the balance. A secondary, more expected feature, is the increased importance of anthropogenic heat flux as an input in winter.

ACKNOWLEDGEMENTS

Special thanks are due to Drs T. R. Oke, C. J. Souch, H. A. Cleugh and H. P. Schmid for useful discussion. This work was supported by grants to Dr T. R. Oke by the Canada Department of Environment (Atmospheric Environment Service) and the Natural Sciences and Engineering Research Council of Canada. The field site and data for anthropogenic heat flux calculations were made available by BC Hydro. Data for anthropogenic heat flux calculations also were made available from City of Vancouver Traffic Department, Vancouver School Board and Vancouver Parks Board.

APPENDIX I: SURFACE DATA BASE

Surface parameter values were calculated using a computerized data base and accessing system that was developed for this study. A parameter can be assessed in response to different source area shapes as meteorological conditions change.

Data base

The requirements of the data base were that the individual grid squares of information would allow the influence of small differences in location of the area boundaries to be identified, but not so small that the effort required to gather the necessary information was unrealistic. These requirements were deemed met by using 100×100 m squares, and data were collected for a 5-km-radius circle centred on the tower (i.e. approximately 8000 squares). The choice of a 5-km circle was based on the areal limits of SAM. Each square was assigned an X and Y coordinate between -50 and $+50$ (no zero).

The Greater Vancouver Regional District 1:2500 land use maps, which have the land use for individual properties, for the Municipalities of Burnaby (1980), Richmond (1980) and the City of Vancouver (1983) were used as the initial data source. Additional information was gathered from Canada Statistics (1987) for the 1986 census, aerial photographs (Vancouver City Planning Department, 1985, scale 1:2500), and visual inspection. The areal extent of surface types within a property were determined from City of Vancouver By-Laws (Vancouver City 1987); facilities within each park from Vancouver Board of Parks and Recreation (1986) and Hickok (1977); data for schools from Vancouver School Board (1982); and aerial photographs (Vancouver City Planning Department, 1985). Further information was calculated and added for the modelling of individual fluxes; i.e. sub-databases were generated for the calculation of specific fluxes.

The data base was compared with a previous detailed surface description conducted by Grimmond (1983) for the Hudson Catchment; a 21-ha area approximately 4·5 km west of the Sunset Tower. The surface characteristics were found to agree very closely. The population calculated from the data base also corresponded very closely to that for individual census tracts.

A second more detailed surface survey was conducted of 10 blocks near the tower. For each 1×1 m square the surface type and height were determined. The information included: vegetation type; vegetation type beneath; shape of vegetation; building type; roof type; and paved surface materials. The information was gathered from visual surveys and aerial photographs (Vancouver City Planning Department, 1985, scale 1:2500).

Accessing system

A modified version of SAM, which incorporated an extension to stable conditions using Gryning *et al.* (1987), was used to calculate hourly dimensions of the nine source-area ellipses: *a* (distance to the upwind edge of the source area), $b+c$ (length of the source area), and d (half the width of the source area) dimensions (see Schmid and Oke, 1990, Figure 5). These are used with the mean wind direction (φ) by the surface data base accessing system to identify which grid squares to use for calculating surface parameters.

To calculate the data base coordinates of an elliptical source area it is necessary to first identify the boundaries when it is aligned with the x axis because, by definition, an ellipse has to have its longest axis parallel to either the x or y axis (Draper and Klingman, 1972). The $b+c$ axis is initially assumed to be aligned along the x axis (90°). The unrotated Y values (Y_{90}) are calculated for X values (X_{90}) from minimum (a) to maximum ($a+b+c$) in steps. The step size can be varied. The smaller the step the better the fit but the greater the computational time. If $b+c$ is the longest axis then the calculation is conducted as follows:

$$Y_{90}=(d^2-(d^2\{[X_{90}-(a+b)]^2/b^2\}))^{0.5} \tag{A1}$$

If the d axis is the longest then d is replaced by b and vice versa in equation (A1).

The located points on the boundaries are then rotated so that the $b+c$ axis is aligned with φ. As the ellipse is symmetrical about the x axis the rotation can be calculated using the same equations, first with $a+Y_{90}$ and second with $a - Y_{90}$ value.

$$X=(\cos(\varphi-90)X_{90}+\sin(\varphi-90)\,Y_{90})/\mathrm{SQS}_x$$

$$Y=(\cos(\varphi-90)\,Y_{90}-\sin(\varphi-90)X_{90})/\mathrm{SQS}_y$$

where SQS_x and SQS_y are the grid dimensions (m). Only the maximum and minimum Y coordinates are stored for each X coordinate. Note that the surface parameter value is determined from the mean of the nine mean values, i.e. a mean value is determined between each ellipse and then for the composite ellipse. Thus areas closer to the tower have proportionally a greater influence than those further away.

For each geometric shape the number of X coordinates (or lines of coordinate data), and the maximum and minimum value of Y for each X is stored for each hour. Once the grid coordinates are identified the required information from the data base can be accessed and the value of the surface parameter calculated. The coordinate finding subroutines also can be linked to the process calculation programs. Since the same coordinates were used several times they were stored for future use.

APPENDIX II: ANTHROPOGENIC HEAT FLUX CALCULATION METHODS

Anthropogenic heat flux components

Q_F is approximated utilizing parameters determined for each hourly weighted source area (section on Modelled fluxes and Appendix I). Q_F is composed of three components (equation (6), Table AII.1).

(i) Q_{FV} is a function of the type and amount of gasoline used, the number of vehicles (n_V) travelling within the source area, the distance they travel, and the fuel efficiency of the vehicles (distance travelled per unit of gasoline). In British Columbia three types of fuel are commonly used (Table AII.2). For fuel economy a value representative for all vehicle types found in a city of 11253 m l^{-1} (Whitford, 1984) was used. Figure AII.1 illustrates n_V profiles for the study area for the major and minor roads.

(ii) In the study area, the two fuels that contribute to Q_{FH} are electricity and gas; other fuels were considered to be negligible and were ignored. Two scales of data were available to enable the calculation of Q_{FH}. Firstly, data at the individual property (consumer) scale were available for 600 consumers within close proximity to the measurement tower. The data were stratified by premise class: single family dwelling, apartments, institutional (further subdivided into schools, churches, hospitals, etc.), industrial, etc., and were available in 2-monthly billing period intervals with no indication of hourly use. Secondly, the only available information showing hourly variation in consumption of electricity and gas was aggregated at much larger scales for the two grid systems. Hourly variation of the consumer-scale heat release was apportioned using the grid fluctuations. BC Hydro provided the gas and electricity data at the two scales (grid and consumer).

(iii) To calculate Q_{FM} the day was subdivided into two time periods: 'active' (0700–2300 h) and 'sleep' (2300–0700 h). For people the metabolic rates from Oke (1978) were used. The number of animals was

Table AII.1. Equations used to calculate the three components of Q_F

	Equation	Symbols	
Q_{FV}	$Q_{FV}=[(n_{Vi}(t)D_{Vi})EV]/[A\ 3600]$ $EV=(\mathrm{NHC}_j\rho_j\mathrm{WFS}_j)/FE$	A—source area (m^2) i—road type (major or minor) n_{Vi}—number of vehicles D_{Vi}—length of road EV—energy used per vehicle (J m^{-1})	t—time (h) j—fuel type NHC$_j$—net heat combustion (J kg^{-1}) ρ_j—density of fuel (kg l^{-1}) WFS$_j$—weighting of fuel sales FE—mean fuel economy (m l^{-1})
Q_{FH}	$Q_{FH}=[(GR_E(t)\Sigma(n_{Ei}C_{Ei}))$ $+((GR_G(t)\Sigma(n_{Gi}C_{Gi})GEF)/3600)]/A$	n—number of consumers C—total mean consumption per individual consumer	i—premise class GR(t)—grid consumption $\Sigma gr(t)$—total grid consumption for study period
	$GR(t)=gr(t)/\Sigma gr(t)$	GEF—gas efficiency (0·675) (electricity = 1·00)	E, G—electricity (W), gas (J)
Q_{FM}	$Q_{FM}=[(nM(t)]/A$	M—metabolic rate (W)	n—number of people and animals

Table AII.2. Fuel consumption, density and net heat combustion (sources: *Oilweek*, 21 September 1987; Shell Canada Ltd. personal communication, 1988)

Fuel type	Consumption in BC January–June 1987 (Ml)	Consumption (per cent)	Density range[a] (kg m^{-3})	Net heat combustion (MJ kg^{-1})
Premium unleaded	185·8	11·03	740–770 (755)	44·33
Regular unleaded	621·1	36·86	720–740 (730)	44·86
Regular leaded	878·1	52·11	710–730 (720)	45·07

[a] Gasoline density varies with fuel mix and season—the midpoint value (in parenthesis) was used

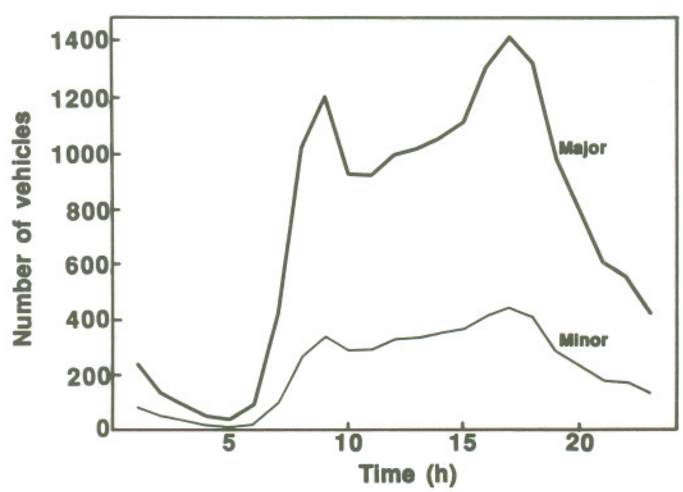

Figure AII.1. Mean profiles of traffic counts for major and minor roads in the study area. (Data source: City of Vancouver Traffic Department, traffic counts) assumed to be 10 per cent of the people and their metabolic rate was set to approximately 25 per cent of people (Bach, 1970).

Method for calculation of the effect of Q_F on surface temperature

The mean maximum hourly Q_{FM} and Q_{FH} are calculated for a time period (units of joules) for an individual 'mean' premise. The summed Q_{FM} and Q_{FH} are reduced by 30 per cent because of air leakage heat losses from buildings (Canadian General Standards Board, 1980). The surface area of the buildings is calculated and used to determine a mean flux density (W m^{-2}) loss from within the buildings. Using values assigned for the heat capacity of the building fabrics and building thicknesses the change in external surface temperature can be calculated. The effect on $L\uparrow$ is calculated and the net effect on Q^* determined.

REFERENCES

Bach, W. 1970. 'An urban circulation model', *Arch. Meteorol. Geophys. Bioklimatol. Ser B.*, **18,** 155–168.

Canada Statistics 1987. *Census of Canada 1986, Enumeration data,* Census Division, Ottawa.

Canada General Standards Board 1980. *Handbook on Insulating Homes for Energy Conservation.* Canadian Government Publishing Centre, Ottawa, 51-GP-42 MP.

Cleugh, H. A. 1990. *Development and evaluation of a regional evaporation model: a study of surface and atmospheric controls on the suburban evaporation regime.* Unpublished PhD thesis, University of British Columbia, Vancouver, 249 pp.

Cleugh, H. A. and Oke, T. R. 1986. 'Suburban–rural energy balance comparisons in summer for Vancouver, B.C.; *Bound Lay. Meteorol.*, **36,** 351–369.

Draper, J. E. and Klingman, J. S. 1972. *Mathematical Analysis,* 2nd edn, Harper & Row, New York, 691 pp.

Fritschen, L. J. and Gay, L. W. 1979. *Environmental Instrumentation,* Springer-Verlag, New York, 216 pp.

Greater Vancouver Regional District 1980. *Land Use Maps for Burnaby,* Scale 1:2500.

Greater Vancouver Regional District 1980. *Land Use Maps for Richmond,* Scale 1:2500.

Greater Vancouver Regional District 1983: *Land Use Maps for Vancouver,* Scale 1:2500.

Grimmond, C. S. B. 1983. *The Suburban water balance: daily, monthly and annual results from Vancouver, B.C.,* Unpublished MSc thesis, The University of British Columbia, Vancouver, 172 pp.

Grimmond, C. S. B., Cleugh, H. A. and Oke, T. R., 1991, 'An objective hysteresis model for urban storage heat flux and its comparison with other schemes', *Atmos. Environ.* **25B,** 311–326.

Grimmond, C. S. B. and Oke, T. R. 1991. 'An evaporation–interception model for urban areas', *Water Resour. Res.* **27,** 1739–1755.

Gryning, S. E., Holtslag, A. A. M., Irwin, J. S. and Sivertsen, D. 1987. 'Applied dispersion modelling based on meteorological scaling parameters', *Atmos. Environ.* **21,** 79–89.

Hay, J. E. and Oke, T. R. 1976. *The Climate of Vancouver,* Tantalus Research Limited, Vancouver, 49 pp.

Henderson-Sellers, B. 1984. 'A new formula for latent heat of vaporization of water as a function of temperature', *Q. J. R. Meteorol. Soc.*, **110,** 1186–1190.

Hickok, R. 1977. *New Encyclopedia of Sports,* McGraw-Hill, New York, 544 pp.

Kalanda, B. D. 1979. *Suburban evaporation estimates in Vancouver,* Unpublished MSc thesis, University of British Columbia, Vancouver, 123 pp.

Kalanda, B. D., Oke, T. R. and Spittlehouse, D. L. 1980, 'Suburban energy balance estimates for Vancouver, B.C. using Bowen Ratio energy-balance approach. *J. Appl. Meteorol.*, **19,** 791–802.

Kalma, J. D. 1974. 'An advective boundary-layer model applied to Sydney, Australia', *Bound. Lay. Meteorol.*, **6,** 351–361.

Kerschgens, M. J. and Drauschke, R. L. 1986. 'On the energy budget of a wintry mid-latitude city atmosphere', *Contrib. Atmos. Phys.*, **59,** 115–125.

Latimer, J. R. 1972. 'Radiation measurement', *Int. Field Year for the Great Lakes Tech. Manual Ser.*, **2,** NRC/USNAS/IHD, Ottawa, 53 pp.

Lowe, P. R. 1977. 'An approximating polynomial for the computation of saturation water vapour pressure', *J. Appl. Meteorol.*, **16,** 100–103.

Mark, D. M. and Church, M. 1977. 'On the misuse of regression in earth science', *Math. Geol.*, **9,** 63–75.

McCaughey, J. H., Mullins, D. W. and Publicover, M. 1987. 'Comparative performance of two reversing Bowen Ratio measurement systems', *J. Atmos. Ocean. Technol.* **4,** 724–730.

Oke, T. R. 1978. *Boundary-layer Climates,* Methuen, London, 372 pp.

Oke, T. R. 1982. 'The energetic basis of the urban heat island', *Q. J. R. Meteorol. Soc.*, **108,** 1–24.

Oke, T. R. 1984. 'Methods in urban climatology', In Kirchhofer, W., Ohmura, A. and Wanner, W. (eds.), *Applied Climatology,* Zurcher Geog. Schriften 14, ETH, Zurich, pp. 19–29.

Oke, T. R. 1988. 'The urban energy balance', *Prog. Phys. Geogr.*, **12,** 471–508.

Oke, T. R. and McCaughey, J. H. 1983. 'Suburban–rural energy balance comparisons for Vancouver, B.C.: an extreme case?', *Bound. Lay. Meteorol.* **26,** 337–354.

Oke, T. R., Kalanda, B. D. and Steyn, D. G. 1981. 'Parameterisation of heat storage in urban areas', *Urban Ecol.*, **5,** 45–54.

Oke, T. R., Cleugh, H. A., Grimmond, C. S. B., Schmid, H. P. and Roth, M. 1989. 'Evaluation of spatially-averaged fluxes of heat, mass and momentum in the urban boundary layer', *Wea. Climate,* **9,** 14–21.

Pasquill, F. 1972. 'Some aspects of boundary layer description', *Q. J. R. Meteorol Soc.*, **98,** 469–494.

Roth, M., Oke, T. R. and Steyn, D. G. 1989. 'Velocity and temperature spectra and cospectra in an unstable suburban atmosphere', *Bound. Lay. Meteorol.* **47,** 309–320.

Schmid, H. P. and Oke, T. R. 1990. 'A model to estimate the source area contributing to surface layer turbulence at a point over a patchy surface', *Q. J. R. Meteorol. Soc.*, **116** (494), 965–988.

Schmid, H. P., Cleugh, H. A., Grimmond, C. S. B. and Oke, T. R. 1991. 'Spatial variability of energy fluxes in suburban terrain', *Bound. Lay. Meteorol.*, **54,** 249–276.

Steyn, D. G. 1980. *Turbulence, diffusion and daytime mixed layer depth over a coastal city*, Unpublished PhD thesis, University of British Columbia, Vancouver, 161 pp.

Steyn, D. G. 1985. 'An objective method to achieve closure of overdetermined surface energy budgets', *Bound. Lay. Meteorol.*, **33,** 303–310.

Steyn, D. G. and Faulkner, D. A. 1986. 'The climatology of sea-breezes in the Lower Fraser Valley, B.C.', *Climate Bull.*, **20,** 21–39.

Steyn, D. G. and McKendry, I. 1988. 'Quantitative and qualitative evaluation of a 3 dimensional mesoscale numerical model simulation of a sea breeze in complex terrain', *Mon. Wea. Rev.*, **116,** 1914–1926.

Steyn, D. G. and Oke, T. R. 1982. 'The depth of the daytime mixed layer at two coastal sites: a model and its validation', *Bound. Lay. Meteorol.*, **24,** 161–180.

Vancouver Board of Parks and Recreation 1986. *Parks and Facilities Chart, General Information*, 16 pp.

Vancouver City 1987. *Zoning and Development By-Law No. 3573.*

Vancouver City Planning Department 1985. Aerial photographs, scale 1:2500.

Vacouver School Board 1982. *Facilities Services*, 2 pp.

Whitford, R. K. 1984. Energy efficient autos: progress and prognosis. In Hollander, J. M. and M. Brooks (eds), *Annual Review of Energy*, vol. 9, 375–408.